

# A Fluid Model with Finite Larmor Radius Effects for Nonlinear Mirror Modes

T. Passot and P.L. Sulem

CNRS, Observatoire de la Côte d'Azur, B.P. 4229, 06304 Nice Cedex 4, France

**Abstract.** A fluid model retaining finite Larmor radius effects and Landau damping is constructed to describe the dynamics of mirror modes in a homogeneous plasma permeated by a strong magnetic field. In order to deal with a model as simple as possible, the fluid hierarchy is closed at the level of the pressure tensor, under the assumption of small deviation from isothermality. Capturing the arrest of the instability at small scales, this model accurately reproduces predictions of the kinetic theory for the mirror instability, including in the regime of warm electrons for which new results are presented. The dispersion relation of kinetic Alfvén waves is also recovered. This model should provide an efficient tool for numerical simulations of the structures and the turbulence that develop in the nonlinear regime.

## 1. Introduction

The presence of mirror modes has been reported in various space plasma environments, such as the solar wind and the magnetospheres of solar system planets, in regions with a high  $\beta$  (ratio of thermal to magnetic pressures) and a strong anisotropy of the proton temperature (dominant in the transverse direction). We refer to *Treumann et al.* [2004] and *Pokhotelov et al.* [2004] for extended references to observational investigations. The multispacecraft observations of the Cluster mission have provided an unambiguous detection of mirror modes in the magnetosheath by permitting a distinction between spatial and temporal variations. These extremely low-frequency waves are associated with strong depressions of the magnetic field (magnetic holes) that are anticorrelated with the plasma density and propagate very slowly in directions almost perpendicular to the ambient field (see e.g. *Lacombe et al.* [1992], *Leckband et al.* [1995], *Schwartz et al.* [1996], *Stasiewicz* [2004]). Recent analysis by *Sahraoui et al.* [2004, 2005] of turbulent magnetic spectra observed in the magnetosheath indicate that their low frequency part is dominated by mirror modes with wave vectors quasi-perpendicular to the ambient magnetic field, the magnetic energy appearing to be injected at a spatial scale associated with the maximum growth rate of the mirror instability. This leads to the picture of a large mirror structure almost stationary in the plasma frame, acting as a pumping source for a nonlinear energy cascade extending up to a few ion Larmor radii.

As noted by *Treumann et al.* [2004], there exists so far no reliable nonlinear theory for the formation and evolution of the mirror modes in high temperature plasmas. An interesting phenomenological description of the mirror instability is given by *Southwood and Kivelson* [1993] and comparisons with hybrid simulations are presented by *McKean et al.* [1992,1993]. Simple saturated solutions based on the conservation of the energy and magnetic moment of the particles are discussed by *Kivelson and Southwood* [1996] and *Pantellini* [1998]. An analogy between mirror instability and superconductiv-

ity is presented by *Treumann et al.* [2004] who predict a scaling law for the variation of the critical magnetic field with the temperature anisotropy. We also mention that *Stasiewicz* [2004, 2005] interprets the magnetosheath structures usually considered as mirror modes, as trains of slow-mode magnetosonic solitons defined as exact solutions of Hall-MHD equations with anisotropic pressure and negligible gyroviscosity. The relevance of such a description for the terrestrial magnetosphere can however be questioned, due to the small-scale character of the structures and the high values of the plasma  $\beta$  that strengthen the importance of kinetic effects.

Although particle trapping certainly plays a role in the saturation of the mirror instability (*Galland Kiverson and Southwood* [1996], (*Pantellini* [1998])), it is of interest to first focus on the role of hydrodynamic nonlinearities that may be at the origin of the observed turbulent spectra. Nevertheless, a specific property of the mirror modes that makes their description difficult using fluid models, originates from the increase of the maximal instability growth rate with the transverse wave number up to a scale comparable with the ion Larmor radius. As a consequence, in spite of the accurate estimates of the large-scale instability growth rate obtained by *Snyder et al.* [1997] and *Bugnon et al.* [2005] using fluid models with Landau damping (Landau fluids), numerical integrations in the nonlinear regime are hardly feasible in the presence of the mirror instability because the smallest scales retained by the spatial discretization turn out to be the most unstable. Improved Landau fluid models including small-scale finite Larmor radius (FLR) corrections are thus necessary to capture the quenching of the instability at these scales. The main goal of this paper is to develop such a model, where nongyrotropic contributions are evaluated in the framework of the linear kinetic theory and included in a convenient way within a Landau fluid description. Such an approach involving nonlinear fluid equations together with the evaluation of suitable quantities using the linear kinetic theory, was used by *Smolyakov et al.* [1995] and *Cheng and Johnson* [1999]. The present model, that allows for an accurate description of quasi-transverse dynamics, appears to be as simple as possible in the sense that the fluid hierarchy is closed at the level of the pressure tensor. Even though it allows for adiabatic behavior, it is best suited for the simulation of quasi-isothermal dynamics since only linearized temperature fluctuations are taken into account.

In order to validate the model, comparisons with the full kinetic theory are performed at the level of the linear mirror instability. This instability was extensively investigated by *Pokhotelov* and coworkers. We nevertheless revisit it here, with two main goals: (i) we evaluate the accuracy of various approximations used in the literature, concerning the plasma response function and the truncation of the kinetic formulas to the dominant order in the direction parameter  $k_z/k_\perp$ ; (ii) we investigate the effect of warm electrons, a regime that was considered by *Pokhotelov et al.* [2000] in the context of a large-scale analysis only. Detailed comparisons are in particular performed with *Pokhotelov et al.* [2004] who studied the stability of modes with wavelengths extending to and beyond the ion Larmor radius in the case of cold electrons. For a closer contact with the fluid theory, we perform the linear stability analysis without introducing the dielectric tensor, as usually done, but rather directly deal with Maxwell equations supplemented by the expressions for the kinetic expressions for the densities and velocities of the ions and electrons.

Because of their very low frequency  $\omega$ , mirror modes

are conveniently analyzed in the framework of a perturbative expansion of the particle distribution functions in terms of the small parameter  $\omega/\Omega$ , where  $\Omega$  denotes the ion gyrofrequency. All the contributions arising beyond the leading order have in fact an unequal influence on the instability growth rate, which leads us to select those terms which are to be retained in the Landau fluid description.

In addition to the computation of the mirror instability growth rate for perturbations with arbitrary transverse scale, the present model accurately reproduces the kinetic Alfvén wave dispersion relation and the phase velocity of oblique magnetosonic waves. Capturing the full dispersion relation of magnetosonic and Alfvén waves whose propagation direction makes an intermediate angle with the magnetic field would require a higher order closure and, as a consequence, a more refined matching of the fluid and kinetic theories.

The outline of the paper is as follow. In Section 2, we use the linearized Vlasov-Maxwell system to compute the dispersion relation of low frequency modes with a direction quasi-perpendicular to the ambient field, in a form valid for small transverse scales and hot electrons, a regime that was not previously addressed in the literature. Section 3 presents an analysis of this dispersion relation, including comparisons with previous work and investigations of yet unexplored regimes. Section 4 is devoted to the derivation of the fluid model together with its validation by comparison with the results of Section 3. Section 5 is a brief conclusion.

## 2. Low Frequency Linear Kinetic Theory

Consider a spatially homogeneous uniformly magnetized plasma with a bi-Maxwellian distribution function at equilibrium

$$f_r^{(0)} = \frac{1}{(2\pi)^{3/2}} \frac{m_r^{3/2}}{T_{\perp r}^{(0)} T_{\parallel r}^{(0)1/2}} \exp \left\{ - \left( \frac{m_r}{2T_{\parallel r}^{(0)}} v_{\parallel}^2 + \frac{m_r}{2T_{\perp r}^{(0)}} v_{\perp}^2 \right) \right\}$$

for the particles of species  $r$  with charge  $q_r$ , mass  $m_r$ , and average number density  $n_r$ , in the absence of net charges or currents. The Vlasov equation for each species is linearized about  $f_r^{(0)}$ , writing  $f_r = f_r^{(0)} + f_r^{(1)}$ , with  $B = B_0 \hat{z} + b^{(1)}$  and  $E = E^{(1)}$ . To simplify the writing, the superscript (1) will be removed in the writing of the individual components of the electric and magnetic fields. The Vlasov equation is supplemented by Maxwell equations that express the electric and magnetic fields  $E$  and  $B$  in terms of the current  $j = \sum_r q_r n_r \int v f_r d^3v$  and the total charge  $\nu = \sum_r q_r n_r \int f_r d^3v$ , in the usual form  $\partial_t B = -c \nabla \times E$ ,  $c \nabla \times B = 4\pi j + \partial_t E$  and  $\nabla \cdot E = 4\pi \nu$ .

It is usual to introduce the scalar potentials  $\Phi$  and  $\Psi$  together with the vector potential  $A$  in the form  $E_{\perp} = -\nabla_{\perp} \Phi - (1/c) \partial_t A_{\perp}$ ,  $E_z = -\partial_z \Psi$  and  $B = B_0 + \nabla \times A$  with  $\nabla \cdot A = 0$ . It follows that  $A_z = (ck_z/\omega)(\Phi - \Psi)$ , where, since there is no ambiguity, we use the same notation for a field and its Fourier transform.

Assuming a plasma made of protons (subscript p) and electrons (subscript e) with charge  $q_p = -q_e = e$ , one rewrites the Ampère-Maxwell equation in the non dimensional form

$$\frac{c_A^2}{c^2} b \left( 1 + \frac{k_z^2}{k_{\perp}^2} \right) \frac{e\Phi}{T_{\perp p}^{(0)}} = \frac{n_p}{n^{(0)}} - \frac{n_e}{n^{(0)}}. \quad (1)$$

Here  $b = T_{\perp p}^{(0)} k_{\perp}^2 / (m_p \Omega^2)$ , where  $\Omega = eB_0 / (m_p c)$  denotes

the proton gyrofrequency, and  $c_A = B_0/\sqrt{4\pi m_p n^{(0)}}$  is the Alfvén speed. Assuming  $c_A \ll c$  implies local electric neutrality  $n_p = n_e$ . Under this assumption, one can also neglect the displacement current and get

$$k^2(\Phi - \Psi) = -\frac{4\pi}{c^2} \frac{\omega}{k_z} j_z. \quad (2)$$

One also has

$$k^2 b_z = i \frac{4\pi}{c} \vec{k}_\perp \times \vec{j}_\perp, \quad (3)$$

where the ion and electron densities and velocities needed to express the current  $j$  are to be computed using the kinetic theory. The transverse magnetic field components are given by

$$b_x = -\frac{k_x k_z}{k_\perp^2} b_z + i \frac{c}{\omega} k_y k_z \left(1 + \frac{k_z^2}{k_\perp^2}\right) (\Phi - \Psi) \quad (4)$$

$$b_y = -\frac{k_y k_z}{k_\perp^2} b_z - i \frac{c}{\omega} k_x k_z \left(1 + \frac{k_z^2}{k_\perp^2}\right) (\Phi - \Psi). \quad (5)$$

It is convenient to express the velocity  $v$  in a cylindrical coordinate system by defining the azimuthal angle  $\phi = \tan^{-1}(v_y/v_x)$  and writing  $v = (v_\perp \cos \phi, v_\perp \sin \phi, v_\parallel)$  and  $\nabla_v = (\cos \phi \partial_{v_\perp} - (\sin \phi/v_\perp) \partial_\phi \sin \phi, \partial_{v_\perp} + (\cos \phi/v_\perp) \partial_\phi, \partial_{v_\parallel})$ . Restricting ourselves to the case of linear perturbations in the form of plane waves of wavevector  $k = (k_x = k_\perp \cos \psi, k_y = k_\perp \sin \psi, k_z)$ , such that  $E^{(1)} = \widehat{E}^{(1)} \exp(i(k \cdot x - \omega t)) + \text{c.c.}$ ,  $b^{(1)} = \widehat{b}^{(1)} \exp(i(k \cdot x - \omega t)) + \text{c.c.}$  and  $f_r^{(1)} = \widehat{f}_r^{(1)} \exp(i(k \cdot x - \omega t)) + \text{c.c.}$ , and using Faraday-Maxwell equation to write  $\widehat{b}^{(1)} = (c/\omega)(k \times \widehat{E}^{(1)})$ , one has (dropping the hats)

$$\begin{aligned} & -i(\omega - k \cdot v) f_r^{(1)} - \frac{q_r B_0}{m_r c} \frac{\partial f_r^{(1)}}{\partial \phi} = \\ & -\frac{q_r}{m_r} \left[ \left( E^{(1)} \left(1 - \frac{k \cdot v}{\omega}\right) + \frac{k(v \cdot E^{(1)})}{\omega} \right) \cdot \nabla_v f_r^{(1)} \right]. \quad (6) \end{aligned}$$

For a bi-Maxwellian distribution, following *Akhiezer et al.* [1975], we get for protons

$$\begin{aligned} f_p^{(1)} = & -e f_p^{(0)} \sum_{l, n=-\infty}^{+\infty} \frac{J_n(\lambda_p) \exp(i(n-l)(\phi - \psi))}{l\Omega + k_z v_\parallel - \omega} \\ & \left\{ \left[ \frac{1}{T_{\perp p}^{(0)}} + \frac{k_z v_\parallel}{\omega} \left( \frac{1}{T_{\parallel p}^{(0)}} - \frac{1}{T_{\perp p}^{(0)}} \right) \right] \times \right. \\ & \left[ l\Omega \left( 1 + \frac{k_z^2}{k_\perp^2} \right) J_l(\lambda_p) \Phi - \frac{k_z^2}{k_\perp^2} l\Omega J_l(\lambda_p) \Psi - \frac{\omega v_\perp}{k_\perp c} J_l'(\lambda_p) b_z \right] \\ & \left. + \left[ \frac{k_z v_\parallel}{T_{\parallel p}^{(0)}} - \frac{l\Omega k_z v_\parallel}{\omega} \left( \frac{1}{T_{\parallel p}^{(0)}} - \frac{1}{T_{\perp p}^{(0)}} \right) \right] J_l(\lambda_p) \Psi \right\}, \quad (7) \end{aligned}$$

where  $\lambda_p = k_\perp v_\perp / \Omega$  and  $J_l$  is the Bessel function of order  $l$ . A similar equation is obtained for the electrons, by replacing  $m_p$  by  $m_e$  and  $e$  by  $-e$  (including in the gyrotropic frequency). We thus concentrate the analysis on the ions and, in order to simplify the writing, now suppress the subscript  $p$ .

Non dimensional velocities and potentials are introduced by writing  $v_\perp = \tilde{v}_\perp \sqrt{2T_\perp^{(0)}/m}$ ,  $v_\parallel = \tilde{v}_\parallel \sqrt{2T_\parallel^{(0)}/m}$ ,  $\Phi = \tilde{\Phi} T_\perp^{(0)}/e$ ,  $\Psi = \tilde{\Psi} T_\perp^{(0)}/e$ ,  $b_z = B_0 \tilde{b}_z$ . One also defines the parameters  $\alpha = (k_\perp/\Omega) \sqrt{2T_\perp^{(0)}/m}$ , and  $\zeta_l = [(\omega - l\Omega)/|k_z|] \sqrt{m/2T_\parallel^{(0)}}$ . The quantity  $\zeta_0$  will

simply be denoted by  $\zeta$ . The computation of the hydrodynamic moments for the protons (number density  $n_p = n \int f_p d^3v$ , velocity  $u_p = \int v f_p d^3v / \int f_p d^3v$ , pressure tensor  $\mathbf{p}_p = m_p n_p \int (v - u_p) \otimes (v - u_p) f_p d^3v$ ) then involves the estimate of integrals of the form ( $\beta$  and  $\gamma$  are here non negative integers)

$$\begin{aligned} & \int e^{ip\phi} f^{(1)} v_{\parallel}^{\gamma} v_{\perp}^{\beta+1} dv_{\perp} dv_{\parallel} d\phi = 2 \left( \frac{2T_{\parallel}^{(0)}}{m} \right)^{\frac{\gamma}{2}} \left( \frac{2T_{\perp}^{(0)}}{m} \right)^{\frac{\beta}{2}} \\ & e^{ip\psi} \int \sum_{l=-\infty}^{+\infty} \left\{ \sqrt{\frac{2}{b}} J_l'(\alpha \tilde{v}_{\perp}) J_{l-p}(\alpha \tilde{v}_{\perp}) \tilde{v}_{\perp} X_{\gamma}(\zeta_l) \tilde{b}_z \right. \\ & - J_l(\alpha \tilde{v}_{\perp}) J_{l-p}(\alpha \tilde{v}_{\perp}) \frac{l\Omega}{\omega} X_{\gamma}(\zeta_l) \left( \tilde{\Phi} + \frac{k_z^2}{k_{\perp}^2} (\tilde{\Phi} - \tilde{\Psi}) \right) \\ & \left. - Y_{\gamma}(\zeta_l) J_l(\alpha \tilde{v}_{\perp}) J_{l-p}(\alpha \tilde{v}_{\perp}) \left[ \frac{T_{\perp}^{(0)}}{T_{\parallel}^{(0)}} - \frac{l\Omega}{\omega} \left( \frac{T_{\perp}^{(0)}}{T_{\parallel}^{(0)}} - 1 \right) \right] \tilde{\Psi} \right\} \\ & e^{-\tilde{v}_{\perp}^2} \tilde{v}_{\perp}^{\beta+1} d\tilde{v}_{\perp}. \end{aligned} \quad (8)$$

We use the notation

$$X_{\gamma}(\zeta_l) = \zeta Y_{\gamma-1}(\zeta_l) + \left( \frac{T_{\perp}^{(0)}}{T_{\parallel}^{(0)}} - 1 \right) Y_{\gamma}(\zeta_l),$$

where  $Y_{\gamma}(\zeta_l)$  is the analytic continuation on the real axis of the function defined by  $\frac{1}{\sqrt{\pi}} \int_{-\infty}^{+\infty} \frac{e^{-x^2} x^{\gamma+1}}{x - \zeta_l} dx$  for  $\text{Im} \zeta > 0$ . Introducing the plasma dispersion function  $Z(\zeta) = \frac{1}{\sqrt{\pi}} P \int_{-\infty}^{+\infty} \frac{e^{-x^2}}{x - \zeta} dx + i\sqrt{\pi} e^{-\zeta^2}$  and the plasma response function  $R(\zeta) = 1 + \zeta Z(\zeta)$ , one has  $Y_0(\zeta_l) = R(\zeta_l)$  and  $Y_1(\zeta_l) = \zeta_l R(\zeta_l)$ .

In order to evaluate the velocities and density fluctuations needed to derive the dispersion relation, we compute the first moments of  $f^{(1)}$  as expansions in powers of the ratio  $\omega/\Omega$ , assuming  $\omega/\Omega \ll 1$  and  $(k_z/\Omega) \sqrt{2T_{\perp}^{(0)}/m} \ll 1$ , with no condition on the magnitude of  $(k_{\perp}/\Omega) \sqrt{2T_{\perp}^{(0)}/m}$ . It is convenient in the sum involved in the right hand side of Eq. (8) to distinguish the contribution of  $l = 0$  that leads to a singular term, from the contributions of  $l \neq 0$ . Asymptotic expressions for  $X_j(\zeta_l)$  and  $Y_j(\zeta_l)$  for  $l \neq 0$  are needed for  $0 \leq j \leq 1$  and are given in the Appendix, together with a few integrals involving Bessel functions.

One obtains for the perturbations of the number density of the protons

$$\begin{aligned} \frac{n_p^{(1)}}{n_p^{(0)}} &= \left( \Gamma_1(b) - \Gamma_0(b) \right) \left( \frac{T_{\perp p}^{(0)}}{T_{\parallel p}^{(0)}} R(\zeta_p) - 1 \right) \frac{b_z}{B_0} \\ & - \Gamma_0(b) R(\zeta_p) \frac{e\Psi}{T_{\parallel p}^{(0)}} - \frac{e}{T_{\perp p}^{(0)}} \left( 1 - \Gamma_0(b) \right) \left( \Phi + \frac{k_z^2}{k_{\perp}^2} (\Phi - \Psi) \right) \\ & - 2 \sqrt{\frac{2m_p}{T_{\perp p}^{(0)}}} \frac{T_{\perp p}^{(0)} - T_{\parallel p}^{(0)}}{m_p} \frac{k_z^2}{k_{\perp} \Omega} C_0^2(b) \frac{b_z}{B_0} \\ & + 2 \frac{k_z^2}{\Omega^2} \frac{2T_{\perp p}^{(0)} - 3T_{\parallel p}^{(0)}}{m_p} D_0^1(b) \frac{e}{T_{\perp p}^{(0)}} \left( \Phi + \frac{k_z^2}{k_{\perp}^2} (\Phi - \Psi) \right) \\ & - 2 \frac{k_z^2}{\Omega^2} \frac{T_{\perp p}^{(0)} - 2T_{\parallel p}^{(0)}}{m_p} D_0^1(b) \frac{e}{T_{\perp p}^{(0)}} \Psi \end{aligned}$$

$$\begin{aligned}
& +2\sqrt{\frac{2m_p}{T_{\perp p}^{(0)}}}C_0^2(b)\frac{\omega^2}{k_{\perp}\Omega}\frac{b_z}{B_0} \\
& -2D_0^1(b)\frac{\omega^2}{\Omega^2}\frac{e}{T_{\perp p}^{(0)}}\left(\Phi+\frac{k_z^2}{k_{\perp}^2}(\Phi-\Psi)\right), \tag{9}
\end{aligned}$$

where the quantities  $C_s^l(b)$  and  $D_s^l(b)$  are defined as integrals of Bessel functions in the Appendix.

For the electrons, when neglecting contributions of order  $m_e/m_p$ , one simply has

$$\frac{n_e^{(1)}}{n_e^{(0)}} = -\left(\frac{T_{\perp e}^{(0)}}{T_{\parallel e}^{(0)}}R(\zeta_e) - 1\right)\frac{b_z}{B_0} + R(\zeta_e)\frac{e\Psi}{T_{\parallel e}^{(0)}}. \tag{10}$$

The ion parallel velocity is given by

$$\begin{aligned}
u_{zp} = & \frac{T_{\perp p}^{(0)}}{T_{\parallel p}^{(0)}}\frac{\omega}{k_z}R(\zeta_p)\left[\left(\Gamma_1(b)-\Gamma_0(b)\right)\frac{b_z}{B_0}-\Gamma_0(b)R(\zeta_p)\frac{e\Psi}{T_{\perp p}^{(0)}}\right] \\
& -\frac{k_z}{\omega}\frac{T_{\perp p}^{(0)}-T_{\parallel p}^{(0)}}{m_p}\left(1-\Gamma_0(b)\right)\frac{e}{T_{\perp p}^{(0)}}\left(1+\frac{k_z^2}{k_{\perp}^2}\right)(\Phi-\Psi) \\
& +2\sqrt{\frac{2T_{\parallel}^{(0)}}{m}}\sqrt{\frac{T_{\perp}^{(0)}}{T_{\parallel}^{(0)}}}\left(\frac{T_{\perp}^{(0)}}{T_{\parallel}^{(0)}}-2\right)C_0^2(b)\frac{k_z\omega}{k_{\perp}\Omega}\frac{b_z}{B_0} \\
& -D_0^1(b)\left[2\frac{T_{\parallel p}^{(0)}}{m_p}\left(\frac{T_{\perp p}^{(0)}}{T_{\parallel p}^{(0)}}-2\right)\frac{k_z\omega}{\Omega^2}\right. \\
& \left.+6\left(\frac{T_{\parallel p}^{(0)}}{m}\right)^2\left(\frac{T_{\perp p}^{(0)}}{T_{\parallel p}^{(0)}}-1\right)\frac{k_z^3}{\omega\Omega^2}\right]\frac{e}{T_{\perp p}^{(0)}}\left(\Phi+\frac{k_z^2}{k_{\perp}^2}(\Phi-\Psi)\right) \\
& +D_0^1(b)\left[-2\frac{T_{\parallel p}^{(0)}}{m}\frac{k_z\omega}{\Omega^2}\right. \\
& \left.+6\left(\frac{T_{\parallel p}^{(0)}}{m}\right)^2\left(\frac{T_{\perp p}^{(0)}}{T_{\parallel p}^{(0)}}-1\right)\frac{k_z^3}{\omega\Omega^2}\right]\frac{e}{T_{\perp p}^{(0)}}\Psi. \tag{11}
\end{aligned}$$

For the electrons, we have

$$\begin{aligned}
u_{ze} = & -\frac{T_{\perp e}^{(0)}}{T_{\parallel e}^{(0)}}\frac{\omega}{k_z}R(\zeta_e)\left[\frac{b_z}{B_0}-R(\zeta_e)\frac{e\Psi}{T_{\perp e}^{(0)}}\right] \\
& +\frac{k_z}{\omega}\frac{T_{\perp e}^{(0)}-T_{\parallel e}^{(0)}}{m_p}b\frac{e}{T_{\perp p}^{(0)}}\left(1+\frac{k_z^2}{k_{\perp}^2}\right)(\Phi-\Psi). \tag{12}
\end{aligned}$$

The transverse hydrodynamic velocity of each particle species  $r$  is conveniently decomposed into compressible and solenoidal parts by writing

$$\mathbf{u}_{\perp r} = -\nabla_{\perp}\chi_{cr} + \nabla_{\perp} \times (\chi_{sr}\hat{z}). \tag{13}$$

One has for the ions

$$\begin{aligned}
\chi_{sp} = & \frac{1}{\Omega}\frac{T_{\perp p}^{(0)}}{m_p}\left(\Gamma_0(b)-\Gamma_1(b)\right)\left[2\left(\frac{T_{\perp p}^{(0)}}{T_{\parallel p}^{(0)}}R(\zeta_p)-1\right)\frac{b_z}{B_0}\right. \\
& \left.+R(\zeta_p)\frac{e\Psi}{T_{\parallel p}^{(0)}}-\frac{e}{T_{\perp p}^{(0)}}\left(\Phi+\frac{k_z^2}{k_{\perp}^2}(\Phi-\Psi)\right)\right] \\
& -4\frac{T_{\perp p}^{(0)}-T_{\parallel p}^{(0)}}{m_p}\frac{k_z^2}{k_{\perp}^2\Omega}C_1^3(b)\frac{b_z}{B_0}+2\sqrt{\frac{2T_{\perp p}^{(0)}}{m_p}}\frac{k_z^2}{k_{\perp}\Omega^2}\times
\end{aligned}$$

$$\begin{aligned}
& \frac{2T_{\perp p}^{(0)} - 3T_{\parallel p}^{(0)}}{m_p} D_1^2(b) \frac{e}{T_{\perp p}^{(0)}} \left( \Phi + \frac{k_z^2}{k_{\perp}^2} (\Phi - \Psi) \right) \\
& - 2 \sqrt{\frac{2T_{\perp p}^{(0)}}{m_p} \frac{k_z^2}{k_{\perp} \Omega^2} \frac{T_{\perp p}^{(0)} - 2T_{\parallel p}^{(0)}}{m_p} D_1^2(b) \frac{e}{T_{\perp p}^{(0)}} \Psi} \\
& + 4C_1^3(b) \frac{\omega^2}{k_{\perp}^2 \Omega} \frac{b_z}{B_0} \\
& - 2 \sqrt{\frac{2T_{\perp p}^{(0)}}{m_p} D_1^2(b) \frac{\omega^2}{k_{\perp} \Omega^2} \left( \Phi + \frac{k_z^2}{k_{\perp}^2} (\Phi - \Psi) \right)}, \quad (14)
\end{aligned}$$

and

$$\begin{aligned}
\chi_{cp} &= \frac{i\omega}{k_{\perp}^2} \left( \Gamma_0(b) - \Gamma_1(b) \right) \frac{b_z}{B_0} + \left( 1 - \Gamma_0(b) \right) \frac{i}{\omega} \frac{k_z^2}{k_{\perp}^2} \times \\
& \frac{e}{T_{\perp p}^{(0)}} \left[ \frac{T_{\perp p}^{(0)} - T_{\parallel p}^{(0)}}{m_p} \left( 1 + \frac{k_z^2}{k_{\perp}^2} \right) (\Phi - \Psi) \right. \\
& \left. - \frac{\omega^2}{k_z^2} \left( \Phi + \frac{k_z^2}{k_{\perp}^2} (\Phi - \Psi) \right) \right]. \quad (15)
\end{aligned}$$

As discussed below, the terms involving  $D_1^2(b)$  will in fact not be retained when constructing the Landau fluid model.

Similarly, one has for the electrons

$$\begin{aligned}
\chi_{se} &= -\frac{1}{\Omega} \frac{T_{\perp e}^{(0)}}{m_p} \left[ 2 \left( \frac{T_{\perp e}^{(0)}}{T_{\parallel e}^{(0)}} R(\zeta_e) - 1 \right) \frac{b_z}{B_0} \right. \\
& \left. - R(\zeta_e) \frac{e\Psi}{T_{\parallel e}^{(0)}} + \frac{e}{T_{\perp e}^{(0)}} \left( \Phi + \frac{k_z^2}{k_{\perp}^2} (\Phi - \Psi) \right) \right] \\
& - \frac{T_{\perp e}^{(0)} - T_{\parallel e}^{(0)}}{m_p} \frac{k_z^2}{k_{\perp}^2 \Omega} \frac{b_z}{B_0} \quad (16)
\end{aligned}$$

and

$$\chi_{ce} = \frac{i\omega}{k_{\perp}^2} \frac{b_z}{B_0}. \quad (17)$$

### 3. Linear Dynamics of Quasi-Perpendicular Modes

Substituting the expressions for the density and for the parallel and perpendicular velocities provided by the kinetic theory into Eqs. (1)-(3) leads to a system of equations easily solved using a symbolic calculator. The code has been validated by checking the dispersion relations of several waves in various regimes.

#### 3.1. Dispersion Relation of Kinetic Alfvén Waves

We have recovered the well-known dispersion relation  $\omega^2 = k_z^2 v_A^2 \left( 1 + \left( \frac{3}{4} + \frac{T_e^{(0)}}{T_p^{(0)}} \right) b \right)$  of kinetic Alfvén waves (KAWS) in the regime  $b \ll 1$  and for isotropic equilibrium temperatures such that  $\tau \equiv T_{\parallel e}^{(0)}/T_{\parallel p}^{(0)} \gg 1$ . The resolution was performed using the fourth pole approximation of the plasma response function  $R$ . Better agreement is found when  $\beta_{\perp p} \equiv 8\pi p_{\perp p}^{(0)}/B_0^2 \ll 1$  and  $\tau \gg 1$ , excluding however extreme values. An example is shown in Fig. 1 that displays  $\Re(\omega)/k_z v_A$  as a function of  $b$  for  $\beta_{\perp p} = 0.001$ ,  $\tau = 100$  and  $A_p = A_e = 0$  (where the anisotropy factor is defined by  $A_r = T_{\perp r}^{(0)}/T_{\parallel r}^{(0)} - 1$ ), for both the numerical resolution of the dispersion relation

(circles) and the above analytic formula (diamonds). We check the excellent agreement at large scales where the formula is asymptotically exact.

### 3.2. Mirror Mode Instability

The kinetic theory involving various expansions and approximations, it is of interest to compare the mirror instability growth rate as given by the above analysis with results from previous papers in order to point out the main sources of imprecision. Using the dispersion relation obtained with Eqs. (1)-(3), we display in Fig. 2 the mirror mode growth rate  $v_{th,p}\Im(\omega)/k_{\perp}$  as a function of  $\theta = k_z/k_{\perp}$  for the case where  $A_p = 1$ ,  $A_e = 0.2$ ,  $\tau = 1$  and  $\beta_{\perp p} = 2$ , using the full function  $R$  (circles) and its one-pole approximation (crosses), together with the growth rate given by formula (23) from *Pokhotelov et al.* [2000] that is based on the ‘‘quasi-hydrodynamic approximation’’ for the large scale dynamics (diamonds). A significant deviation takes place between the three curves when the growth rate increases. However, neglecting terms proportional to  $\theta^2$  (excepted the term  $4i \cos \psi \frac{T_{\perp p}^{(0)} - T_{\parallel p}^{(0)}}{m_p} \frac{k_z^2}{k_{\perp} \Omega} C_1^3(b) \frac{b_z}{B_0}$  appearing in  $u_{yp}$  which provides a significant contribution) but keeping the full function  $R$ , leads to a growth rate whose values all fall within the circle symbols corresponding to the full calculation. We conclude from these observations that the description is most sensitive to the level of approximation of the plasma response function.

We now address the behavior of the instability growth rate as a function of the parameter  $b$  that measures the ratio of the transverse scale of the perturbation to the proton Larmor radius  $r_p$ . The main result of *Pokhotelov et al.* [2004] concerns the increase of the instability threshold at small wavelength and its disappearance for scales smaller than a fraction of the Larmor radius in the case of cold electrons. In order to simplify the fluid modeling, it is of interest to reconsider this case and in particular to investigate here as well the role of the terms proportional to  $\theta^2$ . Figure 3 displays  $\gamma_{max}/\Omega$ , where  $\gamma_{max}$  is the growth rate maximized over the angle of propagation, as a function of  $k_{\perp} r_p = \sqrt{2}b$  for  $A_p = \beta_{\perp p} = 1.5$  and  $T_e = 0$ . These parameters are those of Fig. 1 of *Pokhotelov et al.* [2004]. In Fig. 3, diamonds and circles correspond to the growth rate calculated from the kinetic dispersion relation with and without terms in  $\theta^2$  respectively, as mentioned for the previous case. It is clear from this picture that these terms can be omitted whatever the value of  $\theta$  and  $b$ . Crosses correspond to the growth rate calculated using a series expansion of the dispersion relation truncated at order  $\zeta^3$ . These values are closer to those given by *Pokhotelov et al.* [2004] using a low order approximation of the function  $R$ . For this case again, it appears that the results are most sensitive to the degree of approximation of the plasma dispersion function. Another remark concerns the value of  $\theta$  at which the growth rate is maximum. We find for  $(k_z/k_{\perp})_{max}$  values of the order of a few tenths that are thus, up to the precision of our graph (not shown), exactly 10 times larger than those displayed in Fig. 3 of *Pokhotelov et al.* [2004] where a typo is suspected. The magnitude of the angle associated with the maximum growth rate is of importance since the expansion used in the calculation of the perturbed distribution function is based on the assumption of small  $\theta$ . The above remark on the irrelevance of the terms proportional to  $\theta^2$  nevertheless ensures the validity of the present calculations.

The case of warm electrons is more delicate. As men-



tioned by *Pokhotelov et al.* [2000], in the limit  $b = 0$  the instability growth rate is very sensitive to the electron temperature anisotropy. The behavior of this instability at small wavelength can in fact hardly be estimated using the present formalism, as the growth rate rapidly reaches values which fall outside the range of the small frequency approximation. We display in Fig. 4 the growth rate (maximized over the propagation angles) for two electron temperature anisotropies, namely  $A_e = 1$  (diamonds) and  $A_e = 1.005$  (circles) when  $A_p = 1.5$ ,  $\tau = 1$  and  $\beta_{\perp p} = 1.5$ . As seen on this graph, the value of  $k_{\perp} r_p$  at which the instability disappears is increased by more than an order of magnitude compared to the case  $A_e = 0$ . This degree of anisotropy appears in fact to be at the limit of validity of the the present ordering.

#### 4. A Fluid Model for Mirror Modes

The idea of the model is to supplement the usual MHD equations with information about the small transverse scales, as provided by the linear kinetic theory, with the aim to arrest the mirror instability at small scale. Different models can be constructed with various levels of complexity. In this paper, we restrict ourselves to the simple framework where the fluid hierarchy is closed at the level of the pressure tensor.

##### 4.1. The Fluid Hierarchy

One defines as usual the proton density  $\rho_p = m_p n_p$ , and neglects terms proportional to  $m_e/m_p$ . The proton and electron velocities are related by  $u_e = u_p - j/(en)$ . The ion pressure tensor is rewritten as the sum  $\mathbf{p}_p = p_{\perp p}(\mathbf{I} - \hat{b} \otimes \hat{b}) + p_{\parallel p} \hat{b} \otimes \hat{b} + \mathbf{\Pi}$  of the gyrotropic and gyroviscous contributions, while the electron pressure is taken gyrotropic and characterized by the parallel and transverse pressures  $p_{\parallel e}$  and  $p_{\perp e}$ . One has the usual equations

$$\partial_t \rho_p + \nabla \cdot (\rho_p u_p) = 0 \quad (18)$$

$$\partial_t u_p + u_p \cdot \nabla u_p + \frac{1}{\rho_p} \nabla \cdot \mathbf{p}_p - \frac{e}{m_p} (E + \frac{1}{c} u_p \times B) = 0 \quad (19)$$

$$E = -\frac{1}{c} \left( u_p - \frac{j}{ne} \right) \times B - \frac{1}{ne} \nabla \cdot \mathbf{p}_e, \quad (20)$$

together with the Faraday-Maxwell equation for the magnetic field.

The above hierarchy is to be closed by prescribing the pressure tensors. At the level of the linear kinetic theory, all the hydrodynamic quantities and in particular the components of the pressure tensor, are given in terms of  $b_z$ ,  $\Phi$  and  $\Psi$  (see Section 4.2). Nevertheless, such expressions that involve the plasma response function (and thus nonlocal operators in the time variable) cannot be conveniently substituted into the fluid equations. In addition, assuming a purely linear description of the pressure tensor would be insufficient to accurately reproduce the nonlinear effects at the origin of the formation of coherent structures and of the development of a turbulent regime.

Note that Eq. (20) neglects electron inertia. This point was questioned in *Pokhotelov et al.* [2000], especially when the electrons are hot. His statement is based on the fact that when substituting the kinetic expression for the pressure within the equation for the electron longitudinal velocity in order to get the potential  $\Psi$ , a cancelation takes place, which requires to retain the acceleration term in spite of its smallness. The resulting

expression for  $\Psi$  provided by Eq. (21) of *Pokotelov* [2000] can in fact be reproduced by substituting the kinetic expression of  $j$  within Eq. (2) (where the l.h.s. turns out to be negligible at large scale). This suggests that Eq. (20) can be kept as it is when used in a fluid description. In fact, comparison with the kinetic theory shows that the resulting error is in fact subdominant compared to that made when using a simple approximation of the plasma response function.

#### 4.2. Kinetic Description of the Pressure Tensors

We hereafter show that one can express the linearized temperature fluctuations (directly related to the gyroviscosity stress tensor in terms of fluid quantities. The analysis makes use of the kinetic description of the pressure tensor. In the linear approximation the elements of the pressure tensor perturbations reduce to  $p_{ij}^{(1)} = n^{(0)} m \int v_i v_j f^{(1)} d^3 v$ . Furthermore,  $\hat{b}_x = b_x/B_0$ ,  $\hat{b}_y = b_y/B_0$  and  $\hat{b}_z = 1$ . One has  $p_{\perp}^{(1)} = n^{(0)} m \int (v_{\perp}^2/2) f^{(1)} d^3 v$  and  $p_{\parallel}^{(1)} = n^{(0)} m \int v_{\parallel}^2 f^{(1)} d^3 v$ , from which one easily derives the parallel and transverse temperature perturbations  $T_{\parallel}^{(1)}/T_{\parallel}^{(0)} = p_{\parallel}^{(1)}/p_{\parallel}^{(0)} - \rho^{(1)}/\rho^{(0)}$  and  $T_{\perp}^{(1)}/T_{\perp}^{(0)} = p_{\perp}^{(1)}/p_{\perp}^{(0)} - \rho^{(1)}/\rho^{(0)}$ . It follows that  $\Pi_{xx} = -\Pi_{yy} = n^{(0)} m \int (v_{\perp}^2/2) f^{(1)} \cos 2\phi d^3 v$ ,  $\Pi_{zz} = 0$ ,  $\Pi_{xy} = n^{(0)} m \int (v_{\perp}^2/2) f^{(1)} \sin 2\phi d^3 v$ ,  $\Pi_{xz} = n^{(0)} m \int v_{\parallel} v_{\perp} f^{(1)} \cos \phi d^3 v + (p_{\perp}^{(0)} - p_{\parallel}^{(0)}) \hat{b}_x$  and  $\Pi_{yz} = n^{(0)} m \int v_{\parallel} v_{\perp} f^{(1)} \sin \phi d^3 v + (p_{\perp}^{(0)} - p_{\parallel}^{(0)}) \hat{b}_y$ . Some technical details concerning the asymptotic calculation of the above quantities are given in the Appendix. We concentrate here on the resulting estimates.

##### 4.2.1. Parallel and Transverse Temperatures

One gets for the parallel and transverse temperatures of the ions

$$\frac{T_{\parallel p}^{(1)}}{T_{\parallel p}^{(0)}} = \left(1 - R(\zeta_p) + 2\zeta_p^2 R(\zeta_p)\right) \frac{T_{\perp p}^{(0)}}{T_{\parallel p}^{(0)}} \times \left[ \left(\Gamma_1(b) - \Gamma_0(b)\right) \frac{b_z}{B_0} - \Gamma_0(b) \frac{e\Psi}{T_{\perp p}^{(0)}} \right] \quad (21)$$

and

$$\begin{aligned} \frac{T_{\perp p}^{(1)}}{T_{\perp p}^{(0)}} &= \left( \frac{T_{\perp p}^{(0)}}{T_{\parallel p}^{(0)}} R(\zeta_p) - 1 \right) \times \\ &\left( -2b\Gamma_1(b) + 2b\Gamma_0(b) - \Gamma_0(b) \right) \frac{b_z}{B_0} \\ &- \left( b\Gamma_1(b) - b\Gamma_0(b) \right) R(\zeta_p) \frac{e\Psi}{T_{\parallel p}^{(0)}} \\ &+ \left( b\Gamma_1(b) - b\Gamma_0(b) \right) \frac{e}{T_{\perp p}^{(0)}} \left( \Phi + \frac{k_z^2}{k_{\perp}^2} (\Phi - \Psi) \right). \end{aligned} \quad (22)$$

Analogous expressions are obtained for the electrons, with the  $\Gamma$ -functions then taken in the  $b = 0$  limit.

##### 4.2.2. Gyroviscous Stress

The kinetic theory gives

$$\begin{aligned} \frac{\Pi_{xx}^{(0)}}{p_{\perp p}^{(0)}} &= -\cos 2\psi \left( b\Gamma_0(b) - \Gamma_1(b) - b\Gamma_1(b) \right) \times \\ &\left[ 2 \left( \frac{T_{\perp p}^{(0)}}{T_{\parallel p}^{(0)}} R(\zeta_p) - 1 \right) \frac{b_z}{B_0} + R(\zeta_p) \frac{e\Psi}{T_{\parallel p}^{(0)}} \right] \end{aligned}$$

$$\begin{aligned}
& -\frac{e}{T_{\perp p}^{(0)}}\left(\Phi + \frac{k_z^2}{k_{\perp}^2}(\Phi - \Psi)\right)] \\
& -\cos 2\psi \Gamma_1(b) \left(\frac{T_{\perp p}^{(0)}}{T_{\parallel p}^{(0)}} R(\zeta_p) - 1\right) \frac{b_z}{B_0} + i \sin 2\psi \frac{k_z}{\Omega} \frac{k_z}{\omega} \times \\
& \frac{e}{T_{\perp p}^{(0)}} \left[ \left(\Gamma_0(b) - \Gamma_1(b)\right) - \frac{1}{b} \left(1 - \Gamma_0(b)\right) \right] \times \\
& \left[ \frac{T_{\perp p}^{(0)} - T_{\parallel p}^{(0)}}{m_p} \left(1 + \frac{k_z^2}{k_{\perp}^2}\right) (\Phi - \Psi) \right. \\
& \left. - \frac{\omega^2}{k_z^2} \left(\Phi + \frac{k_z^2}{k_{\perp}^2}(\Phi - \Psi)\right) \right] \\
& -i \sin 2\psi \frac{\omega}{\Omega} \left[ \frac{1}{b} \left(\Gamma_0(b) - 1 - \Gamma_1(b)\right) \right. \\
& \left. + 2 \left(\Gamma_0(b) - \Gamma_1(b)\right) \right] \frac{b_z}{B_0}. \tag{23}
\end{aligned}$$

One also has

$$\begin{aligned}
\frac{\Pi_{xz}}{p_{\parallel p}^{(0)}} &= i \sin \psi \frac{T_{\perp}^{(0)}}{T_{\parallel}^{(0)}} \frac{k_{\perp}}{\Omega} \frac{\omega}{k_z} \left(\Gamma_0(b) - \Gamma_1(b)\right) \times \\
R(\zeta) &\left(2 \frac{T_{\perp}^{(0)}}{T_{\parallel}^{(0)}} \frac{b_z}{B_0} + \frac{e\Psi}{T_{\parallel}^{(0)}}\right) + \cos \psi \frac{k_z}{k_{\perp}} \left(\frac{T_{\perp}^{(0)}}{T_{\parallel}^{(0)}} - 1\right) \times \\
&\left[ \left(\Gamma_0(b) - \Gamma_1(b) - 1\right) \frac{b_z}{B_0} - \left(1 - \Gamma_0(b)\right) \frac{e\Psi}{T_{\perp}^{(0)}} \right] \\
&- \left[ \cos \psi \left(\frac{T_{\perp}^{(0)}}{T_{\parallel}^{(0)}} - 2\right) \frac{k_z}{k_{\perp}} \left(1 - \Gamma_0(b)\right) \right. \\
& \left. + i \sin \psi \frac{T_{\perp}^{(0)} - T_{\parallel}^{(0)}}{m} \frac{T_{\perp}^{(0)}}{T_{\parallel}^{(0)}} \frac{k_z k_{\perp}}{\omega \Omega} \times \right. \\
& \left. \left(\Gamma_0(b) - \Gamma_1(b) - 1\right) \right] \left(1 + \frac{k_z^2}{k_{\perp}^2}\right) \frac{e}{T_{\perp}^{(0)}} (\Phi - \Psi) \\
& + 4i C_1^3(b) \sin \psi \left(\frac{T_{\perp}^{(0)}}{T_{\parallel}^{(0)}} - 2\right) \frac{k_z \omega}{k_{\perp} \Omega} \frac{b_z}{B_0}. \tag{24}
\end{aligned}$$

The elements  $\Pi_{xy}$  and  $\Pi_{yz}$  are deduced from  $\Pi_{xx}$  and  $\Pi_{xx}$  respectively, by replacing  $\sin 2\psi$  by  $-\cos 2\psi$  and  $\cos 2\psi$  by  $\sin 2\psi$ . Furthermore, the contributions involving  $\Phi - \Psi$  are conveniently expressed in terms of the transverse magnetic field components, using Eqs. (4) and (5).

### 4.3. Modeling Parallel and Transverse Temperatures

The MHD description of plasmas often involves the double adiabatic law of *Chew, Goldberg and Law* [1956], that relates the fluctuations of the gyrotropic pressure components to those of the density and of the magnetic field intensity through specific power law dependencies. The relevance of such a functional dependency with different exponents was recently stressed by *Stasiewicz* [2005] who suggested empirical fittings on the basis of the analysis of observational data provided by the Cluster spacecraft mission, for a broad range of values of the plasma  $\beta$ . A semi-phenomenological approach based on the use of complex polytropic indices calculated as function of the mode properties is presented by *Belmont et al.* [1992]. The analysis is based on the fluid hierarchy for the lowest order moments, supplemented by the kinetic expression of the polytropic indices provided by the kinetic theory as derived by *Belmont and Mazelle* [1992].

In this section, we derive evolution equations for the temperature fluctuations that easily couple with the hy-

drodynamic equations, while they also accurately reproduce the linear kinetic theory. For this purpose, we are led to prescribe

$$T_{\parallel r} = T_{\parallel r}^{(0)}(1 + \alpha_{\parallel r}) \quad (25)$$

$$T_{\perp r} = T_{\perp r}^{(0)} \left( \frac{|B_1|}{B_0} \right)^{-A_r} (1 + \alpha_{\perp r}). \quad (26)$$

Using the expression for the parallel temperatures, one has for the ions

$$\alpha_{\parallel p} = \frac{T_{\perp p}^{(0)}}{T_{\parallel p}^{(0)}} \left( 1 - R(\zeta_p) + 2\zeta_p^2 R(\zeta_p) \right) \times \left[ \left( \Gamma_1(b) - \Gamma_0(b) \right) \frac{b_z}{B_0} - \Gamma_0(b) \frac{e\Psi}{T_{\perp p}^{(0)}} \right] \quad (27)$$

and for the electrons

$$\alpha_{\parallel e} = -\frac{T_{\perp e}^{(0)}}{T_{\parallel e}^{(0)}} \left( 1 - R(\zeta_e) + 2\zeta_e^2 R(\zeta_e) \right) \left( \frac{b_z}{B_0} + \frac{e\Psi}{T_{\perp e}^{(0)}} \right). \quad (28)$$

This model that only retains linearized temperature fluctuations is mostly adapted to the quasi-isothermal dynamics, a regime consistent with the ultra low frequencies of the linear mirror modes. Furthermore, as observed by *Sahraoui et al.* [2005], nonlinear mirror structures prove to be stationary at all scales in the plasma frame.

The plasma response function can easily be eliminated from the above formulas by introducing the hydrodynamic velocities of each species along the ambient field. This gives

$$\alpha_{\parallel p} = \frac{1 - R(\zeta_p) + 2\zeta_p^2 R(\zeta_p)}{\text{sgn}(k_z) \zeta_p R(\zeta_p)} \sqrt{\frac{m_p}{2T_{\parallel p}^{(0)}}} \left[ u_{zp} + \frac{T_{\perp p}^{(0)} - T_{\parallel p}^{(0)}}{m_p} \frac{1 - \Gamma_0(b)}{b} \frac{1}{v_A^2} \frac{j_z}{en^{(0)}} \right] \quad (29)$$

$$\alpha_{\parallel e} = \frac{1 - R(\zeta_e) + 2\zeta_e^2 R(\zeta_e)}{\text{sgn}(k_z) \zeta_e R(\zeta_e)} \sqrt{\frac{m_e}{2T_{\parallel e}^{(0)}}} \left[ u_{ze} - \frac{T_{\perp e}^{(0)} - T_{\parallel e}^{(0)}}{m_p} \frac{1}{v_A^2} \frac{j_z}{en^{(0)}} \right]. \quad (30)$$

If for the sake of simplicity, one restricts oneself to a two-pole approximation of the plasma response function, one gets

$$\alpha_{\parallel p} = -i\sqrt{\pi} \frac{k_z}{|k_z|} \sqrt{\frac{m_p}{2T_{\parallel p}^{(0)}}} \left[ u_{zp} + \frac{T_{\perp p}^{(0)} - T_{\parallel p}^{(0)}}{m_p} \frac{1 - \Gamma_0(b)}{b} \frac{1}{v_A^2} \frac{j_z}{en^{(0)}} \right]$$

$$\alpha_{\parallel e} = -i\sqrt{\pi} \frac{k_z}{|k_z|} \sqrt{\frac{m_e}{2T_{\parallel e}^{(0)}}} \left[ u_{ze} - \frac{T_{\perp e}^{(0)} - T_{\parallel e}^{(0)}}{m_p} \frac{1}{v_A^2} \frac{j_z}{en^{(0)}} \right]$$

that remain finite as  $\zeta_p$  or  $\zeta_e$  become infinite. One easily checks that reproducing the proper decay of the Landau damping in this adiabatic limit [associated with the imaginary part of the ratio involving the  $R$  function in Eqs. (29) and (30)] actually requires the use of at least the three-pole approxi-

mant  $R_3(\zeta) = \frac{2 - i\sqrt{\pi}\zeta}{2 - 3i\sqrt{\pi}\zeta - 4\zeta^2 + 2i\sqrt{\pi}\zeta^3}$ , which yields  $\frac{1 - R(\zeta) + 2\zeta_i^2 R(\zeta)}{\zeta R(\zeta)} \approx \frac{2i\sqrt{\pi}}{-2 + i\sqrt{\pi}\zeta}$ . Substituting in Eqs. (29) and (30) and returning to the physical space for the time and longitudinal coordinate variables, we are led to prescribe  $\alpha_{\parallel p}$  and  $\alpha_{\parallel e}$  as the solutions of the dynamical equations

$$\begin{aligned} & \left( \partial_t - \frac{2}{\sqrt{\pi}} \sqrt{\frac{2T_{\parallel p}^{(0)}}{m_p}} \mathcal{H}_z \partial_z \right) \alpha_{\parallel p} \\ & + 2\partial_z \left[ u_{zp} + \frac{T_{\perp p}^{(0)} - T_{\parallel p}^{(0)}}{m_p} \frac{1 - \Gamma_0(b)}{b} \frac{1}{v_A^2} \frac{j_z}{en^{(0)}} \right] = 0 \quad (31) \\ & \left( \partial_t - \frac{2}{\sqrt{\pi}} \sqrt{\frac{2T_{\parallel e}^{(0)}}{m_e}} \mathcal{H}_z \partial_z \right) \alpha_{\parallel e} \\ & + 2\partial_z \left[ u_{ze} - \frac{T_{\perp e}^{(0)} - T_{\parallel e}^{(0)}}{m_p} \frac{1}{v_A^2} \frac{j_z}{en^{(0)}} \right] = 0. \quad (32) \end{aligned}$$

Turning to the transverse quantities, we write

$$\begin{aligned} \alpha_{\perp p} &= b \left( \Gamma_0(b) - \Gamma_1(b) \right) \left[ 2 \left( \frac{T_{\perp p}^{(0)}}{T_{\parallel i}^{(0)}} R(\zeta_p) - 1 \right) \frac{b_z}{B_0} \right. \\ & + R(\zeta_p) \frac{e\Psi}{T_{\parallel i}^{(0)}} - \frac{e}{T_{\perp i}^{(0)}} \left( \Phi + \frac{k_z^2}{k_{\perp}^2} (\Phi - \Psi) \right) \left. \right] \\ & + \left[ A_p - \Gamma_0(b) \left( \frac{T_{\perp p}^{(0)}}{T_{\parallel p}^{(0)}} R(\zeta_p) - 1 \right) \right] \frac{b_z}{B_0}. \quad (33) \end{aligned}$$

By comparison with the kinetic expression for  $\chi_{sp}$ , we are led to prescribe

$$\alpha_{\perp p} + \Gamma_0(b) \frac{T_{\perp p}^{(0)}}{T_{\parallel p}^{(0)}} R(\zeta_p) \frac{b_z}{B_0} = \frac{k_{\perp}^2}{\Omega} \chi_{sp} + K_p \frac{b_z}{B_0} \quad (34)$$

with

$$K_p = \left( 4C_1^3(b) \frac{T_{\perp p} - T_{\parallel p}}{m_p} \frac{k_z^2}{\Omega^2} + A_p + \Gamma_0(b) \right).$$

When dealing with  $\alpha_{\perp p}$  it is sufficient to replace the plasma response function by its one pole approximation  $R_1(\zeta_p) = 1/(1 - i\sqrt{\pi}\zeta_p)$ . This leads to the dynamical equation

$$\begin{aligned} & \left[ \partial_t - \frac{1}{\sqrt{\pi}} \sqrt{\frac{2T_{\parallel p}^{(0)}}{m_p}} \mathcal{H}_z \partial_z \right] \left( \alpha_{\perp p} - \frac{k_{\perp}^2}{\Omega} \chi_{sp} - K_p \frac{b_z}{B_0} \right) \\ & - \frac{1}{\sqrt{\pi}} \sqrt{\frac{2T_{\parallel p}^{(0)}}{m_p}} \Gamma_0(b) \frac{T_{\perp p}^{(0)}}{T_{\parallel p}^{(0)}} \mathcal{H}_z \partial_z \frac{b_z}{B_0} = 0. \quad (35) \end{aligned}$$

Note that  $-k_{\perp}^2 \chi_{sp}$  identifies with the longitudinal vorticity  $\omega_{zp} = \hat{z} \cdot (\nabla \times u_p)$  of the proton flow.

The equivalent equation for the electrons is simply

$$\begin{aligned} & \left[ \partial_t - \frac{1}{\sqrt{\pi}} \sqrt{\frac{2T_{\parallel e}^{(0)}}{m_e}} \mathcal{H}_z \partial_z \right] \left( \alpha_{\perp e} - (A_e + 1) \frac{b_z}{B_0} \right) \\ & - \frac{1}{\sqrt{\pi}} \sqrt{\frac{2T_{\parallel e}^{(0)}}{m_e}} \frac{T_{\perp e}^{(0)}}{T_{\parallel e}^{(0)}} \mathcal{H}_z \partial_z \frac{b_z}{B_0} = 0. \quad (36) \end{aligned}$$

In the above equation,  $\partial_t b_z$  is expressed using the Faraday equation and the generalized Ohm's law. The above closure equations were derived by a linear analysis. In order to restore Galilean invariance, it may nevertheless be suitable to replace the partial time derivatives  $\partial_t$  acting on the  $\alpha$ 's by the convective derivative  $\partial_t + u \cdot \nabla$ .

As already noted, this model takes into account temperature fluctuations at the linear level only. As a consequence, although it allows for adiabatic behavior, it is best suited for the simulation of quasi-isothermal dynamics.

#### 4.4. Modeling the Gyroviscous Stress

It is convenient to write

$$\frac{1}{p_{\perp p}^{(0)}} \nabla_{\perp} \cdot \mathbf{\Pi}_{\perp} = -\nabla_{\perp} \mathcal{A} + \nabla_{\perp} \times (\mathcal{B} \hat{z}). \quad (37)$$

The quantities  $\mathcal{A}$  and  $\mathcal{B}$  are expressed by means of Eq. (23). At this level, we check that, to leading order in  $k_z^2/k_{\perp}^2$ ,  $\mathcal{A}$  and  $\mathcal{B}$  reduce to the quantities  $-\delta p_c$  and  $-\delta p_s$  of *Cheng and Johnson* [1999], when assuming a zero drift frequency.

Using Eq. (14) in the simplified form where subdominant terms are neglected, together with Eq. (22) that gives

$$\begin{aligned} \left( \frac{T_{\perp p}^{(0)}}{T_{\parallel p}^{(0)}} R(\zeta_p) - 1 \right) \frac{b_z}{B_0} &= \frac{1}{\Gamma_0(b)} \times \\ &\left( k_{\perp}^2 \chi_{sp} + 4 \frac{T_{\perp p}^{(0)} - T_{\parallel p}^{(0)}}{m_p} \frac{k_z^2}{\Omega^2} C_1^3(b) \frac{b_z}{B_0} - \frac{T_{\perp p}^{(1)}}{T_{\perp p}^{(0)}} \right), \end{aligned} \quad (38)$$

we finally obtain

$$\begin{aligned} \mathcal{A} &= \left( 1 - \frac{\Gamma_1(b)}{b[\Gamma_0(b) - \Gamma_1(b)]} + \frac{\Gamma_1(b)}{\Gamma_0(b)} \right) \frac{k_{\perp}^2}{\Omega} \chi_{sp} \\ &- \frac{\Gamma_1(b)}{\Gamma_0(b)} \frac{T_{\perp p}^{(1)}}{T_{\perp p}^{(0)}} \end{aligned} \quad (39)$$

$$\begin{aligned} \mathcal{B} &= -i \frac{\omega}{\Omega} \left[ \frac{\Gamma_0(b) - 1 - \Gamma_1(b)}{b} + 2 \left( \Gamma_0(b) - \Gamma_1(b) \right) \right. \\ &+ \left. \frac{\Gamma_0(b) - \Gamma_1(b)}{1 - \Gamma_0(b)} \left( \Gamma_0(b) - \Gamma_1(b) - \frac{1 - \Gamma_0(b)}{b} \right) \right] \frac{b_z}{B_0} \\ &+ \frac{1}{1 - \Gamma_0(b)} \left[ \Gamma_0(b) - \Gamma_1(b) - \frac{1 - \Gamma_0(b)}{b} \right] \frac{k_{\perp}^2}{\Omega} \chi_{cp}. \end{aligned} \quad (40)$$

In  $\mathcal{A}$ , we have neglected a contribution of the form  $4C_1^3(b) \left( \frac{b\Gamma_0(b) - \Gamma_1(b) - b\Gamma_1(b)}{\Gamma_0(b) - \Gamma_1(b)} + \frac{b\Gamma_1(b)}{\Gamma_0(b)} \right) \frac{T_{\perp p}^{(0)} - T_{\parallel p}^{(0)}}{T_{\perp p}^{(0)}} \frac{k_z^2}{k_{\perp}^2} \frac{b_z}{B_0}$  that, without being totally negligible, is nevertheless relatively small due to the factor  $k_z^2/k_{\perp}^2$ . We check that this term has essentially no effect at the level of the dispersion relation and can thus be discarded in the fluid model. Furthermore, in the above equations, the temperature disturbance  $T_{\perp p}^{(1)}/T_{\perp p}^{(0)}$  is provided by  $\alpha_{\perp p}$ . The quantity  $i\omega b_z/B_0$  is estimated using the Faraday-Maxwell equation and the expressions of  $\Psi$  and  $E_{\perp}$  given by the generalized Ohm's law. Finally, the contributions  $\chi_s$  and  $\chi_c$  are given by  $\chi_s \hat{z} = (ik_{\perp} \times u_{\perp})/k_{\perp}^2$  and  $\chi_c = (ik_{\perp} \cdot u_{\perp})/k_{\perp}^2$ .

Let us now turn to  $\mathbf{\Pi}_z = (\Pi_{xz}, \Pi_{yz}, \Pi_{zz})$  where  $\Pi_{zz} = 0$  in the linear description. This vector was neglected by *Smolyakov et al.* [1995] and *Cheng and Johnson*, [1999], but turns out not to be globally negligible. Writing

$$\mathbf{\Pi}_z = -\nabla_{\perp} \mathcal{C} + \nabla_{\perp} \times (\mathcal{D} \hat{z}), \quad (41)$$

simplified expressions for  $\mathcal{C}$  and  $\mathcal{D}$  can be derived from Eq. (24) by noticing that the contributions involving  $\left(\frac{T_{\perp}^{(0)}}{T_{\parallel}^{(0)}} - 2\right) \frac{k_z}{k_{\perp}} (1 - \Gamma_0(b)) \left(1 + \frac{k_z^2}{k_{\perp}^2}\right) \frac{e}{T_{\perp}^{(0)}} (\Phi - \Psi)$  in Eq.(24) and in the corresponding equation for  $\Pi_{yz}$  are small and also that neglecting the terms proportional to  $\omega$  has a minor influence at the level of the dispersion relation. A more accurate description is possible but would lead to a cumbersome formalism. Retaining the above approximations, we are led to write

$$\frac{\mathcal{C}}{p_{\parallel p}^{(0)}} = i \frac{k_z}{k_{\perp}^2} \left(\frac{T_{\perp}^{(0)}}{T_{\parallel}^{(0)}} - 1\right) \left[ \left(\Gamma_0(b) - \Gamma_1(b) - 1\right) \frac{b_z}{B_0} - \left(1 - \Gamma_0(b)\right) \frac{e\Psi}{T_{\perp}^{(0)}} \right] \quad (42)$$

$$\frac{\mathcal{D}}{p_{\parallel p}^{(0)}} = \left(\Gamma_0(b) - \Gamma_1(b) - 1\right) \left(\frac{T_{\perp}^{(0)}}{T_{\parallel}^{(0)}} - 1\right) \frac{4\pi}{cB_0 k_{\perp}^2} j_z. \quad (43)$$

#### 4.5. Comparison with the Kinetic Theory

In order to test the accuracy of the fluid model, we compare in this section its predictions for the dispersion relation of the various MHD waves, and the instability growth rate of the mirror modes, with the results of Section II, based on the full kinetic theory. Linearizing the fluid model in a reference frame where  $\partial/\partial y = 0$ , one easily derives

$$-\partial_t \partial_{xx} \chi_{cp} + \partial_{xx} \left( \frac{p_{\perp}}{\rho_p^{(0)}} - \frac{p_{\perp}^{(0)}}{\rho_p^{(0)}} \mathcal{A} + c_A^2 \frac{b_z}{B_0} \right) + \left( c_A^2 + \frac{p_{\perp}^{(0)} - p_{\parallel}^{(0)}}{\rho_p^{(0)}} \right) \partial_{zz} \frac{b_z}{B_0} - \frac{p_{\parallel p}^{(0)}}{\rho_p^{(0)}} \partial_{xxz} \mathcal{C} = 0 \quad (44)$$

$$-\partial_t \partial_{xx} \chi_{sp} - \left( c_A^2 + \frac{p_{\perp}^{(0)} - p_{\parallel}^{(0)}}{\rho_p^{(0)}} \right) \partial_{xz} \frac{b_y}{B_0} - \frac{p_{\perp}^{(0)}}{\rho_p^{(0)}} \partial_{xx} \mathcal{B} - \frac{p_{\parallel}^{(0)}}{\rho_p^{(0)}} \partial_{xxz} \mathcal{D} = 0 \quad (45)$$

$$\partial_t u_{zp} + \partial_z \left( \frac{p_{\parallel}}{\rho_p^{(0)}} + \frac{p_{\perp}^{(0)} - p_{\parallel}^{(0)}}{\rho_p^{(0)}} \frac{b_z}{B_0} \right) - \frac{p_{\parallel p}^{(0)}}{\rho_p^{(0)}} \partial_{xx} \mathcal{C} = 0, \quad (46)$$

where the pressures without subscript denote the sum of the proton and electron pressures and where we have used the generalized Ohm's law that rewrites

$$\frac{c}{B_0} E_x = \partial_x \chi_{sp} - \frac{c_A^2}{\Omega} \partial_x \frac{b_z}{B_0} + \left( \frac{c_A^2}{\Omega} + \frac{p_{\perp e}^{(0)} - p_{\parallel e}^{(0)}}{\rho_p^{(0)} \Omega} \right) \partial_z \frac{b_x}{B_0} - \frac{1}{\rho_p^{(0)} \Omega} \partial_x p_{\perp e} \quad (47)$$

$$\frac{c}{B_0} E_y = -\partial_x \chi_{cp} + \left( \frac{c_A^2}{\Omega} + \frac{p_{\perp e}^{(0)} - p_{\parallel e}^{(0)}}{\rho_p^{(0)} \Omega} \right) \partial_z \frac{b_y}{B_0} \quad (48)$$

$$\Psi = \frac{1}{n_0 e} \left( p_{\parallel e} + (p_{\perp e}^{(0)} - p_{\parallel e}^{(0)}) \frac{b_z}{B_0} \right). \quad (49)$$

We also have

$$\partial_t \frac{n_p}{n_0} - \partial_{xx} \chi_{cp} + \partial_z u_{zp} = 0 \quad (50)$$

$$\partial_t \frac{b_y}{B_0} + \frac{c}{B_0} (\partial_z E_x + \partial_{xz} \Psi) = 0 \quad (51)$$

$$\partial_t \frac{b_z}{B_0} + \frac{c}{B_0} \partial_x E_y = 0, \quad (52)$$

together with the relations  $\partial_x b_x + \partial_z b_z = 0$  and  $j_z = \frac{c}{4\pi} \partial_x b_y$ .

Equations (44)-(46) and (50)-(52), supplemented by the expressions for the pressures resulting from Eqs. (31)-(32) and Eqs. (35)-(36), provide a closed system from which the dispersion relation is easily obtained using a symbolic calculator.

In order to test the capability of the model to describe KAWs, we included in Fig. 1 for the frequency of these waves as a function of perpendicular wavenumber, the prediction of the fluid model (cross symbols). We observe that the agreement with the kinetic theory is excellent.

Concerning magneto-sonic waves propagating perpendicular to the ambient magnetic field, the phase velocity is accurately reproduced by the model, since the adiabatic regime associated with the condition  $\partial_t \gg \partial_z$  is correctly described by the dynamical equations (31)-(32) and (35)-(36) governing the pressures. The corrective dispersive terms in the wavenumber cone  $k_z/k_\perp \ll 1$  which require second order accuracy in a  $1/\Omega$  expansion of the FLR terms, are however not properly captured. The kinetic theory developed in the previous section is also insufficient to describe this finite frequency mode that requires higher order terms in the development of  $X_\gamma$  and  $Y_\gamma$ . In fact, only a few terms proportional to  $\omega^4/\Omega^4$  are to be calculated, that originate from the next order contribution to  $X_0$ , the other extra terms in  $Y_0$ ,  $X_1$  and  $Y_1$  being all proportional to  $k_z$ . These terms give rise to an extra contribution to  $n_p^{(1)}/n_p^{(0)}$  that reads  $\frac{2}{b} (b\Gamma_0(b) - b\Gamma_1(b) - \Gamma_1(b)) \frac{\omega^4}{\Omega^4} \frac{b_z}{B_0}$  and to an extra contribution to  $u_{yp}$  (taking the angle  $\psi = 0$ ) given by

$$-2i \sqrt{\frac{2T_{\perp p}^{(0)}}{m_p}} \sqrt{\frac{2}{b}} \left( b\Gamma_1(b) - b\Gamma_0(b) + \Gamma_1(b) + \frac{\Gamma_1(b)}{2b} \right) \frac{\omega^4}{\Omega^4} \frac{b_z}{B_0}.$$

The integrals are here calculated keeping only the  $l = \pm 1$  terms in the summation (see Appendix). The other terms of the series contribute for only a few percents when  $b = O(1)$ . With these extra terms, one easily computes the dispersion relation of transverse magnetosonic waves and verifies its agreement with eqs. (2.10)-(2.11) of *Mikhailovskii and Smolyakov* [1985]. Figure 5 displays  $\Re(\omega)/k_\perp v_A$  as a function of  $b$  for  $\beta_{\parallel p} = 1$ ,  $\tau = 1$  and  $A_p = A_e = 0$  (taking  $\theta = 10^{-4}$ ) for the numerical resolution of the dispersion relation of the full kinetic theory (diamonds), for the analytic formula of *Mikhailovskii and Smolyakov* [1985] (crosses), which is only valid for very small values of  $b$ , and for the fluid model (circles). As announced, for transverse magnetosonic waves, the fluid model is only valid at the point  $b = 0$ .

We now turn to the main property of this model, i.e. its capability to model of mirror modes at finite values of the parameter  $b$ . We first address a case with cold electrons and parameters corresponding to a proximity to the mirror instability threshold ( $A_p = 0.7$ ,  $\beta_{\perp p} = 1.5$ ,  $\theta = 0.1$ ). As seen on Fig. 6, the agreement between kinetic theory (diamonds) and the fluid model (circles) is excellent, except at the largest values of the parameter  $b$  for which a deviation is visible, although small. In order to analyze the origin of the discrepancy at these small scales, we symbolize by crosses the results obtained when the dispersion relation is derived from the fluid model in an improved form that retains all terms in the FLR corrections and a fourth pole approximation used



for the plasma response function in the first term of  $\Pi_{yz}$ . Note that these extra terms cannot be simply incorporated when the fluid model is used to address an initial value problem, due to the presence of high powers of the frequency in the denominator. They are only used here in the computation of the dispersion relation for comparison. Figure (6) shows that the agreement between kinetic theory and this “extended” fluid model is then excellent throughout the entire  $b$ -range. This suggests that a proper modeling of these extra terms in the framework of a more sophisticated model, would ensure a high accuracy up to the smallest transverse scales. Keeping a larger number of fluid moments could also contribute to improve the accuracy of the model.

For parameters corresponding to a finite distance to threshold and finite electron temperature ( $\tau = 1$ ,  $A_p = 1.5$ ,  $A_e = 0.1$ ,  $\beta_{\perp p} = 1.5$ ,  $\theta = 0.2$ ), we compare in Fig. 7 the results of the kinetic theory (diamonds) with those of the fluid model (circles) for the imaginary part of the frequency as a function of  $k_{\perp} r_p$ . Crosses again correspond to the “extended” fluid model. As seen on this graph, the agreement between kinetic theory and the fluid models is good (and even better when including the extra terms) when the growth rate takes small values. It clearly deteriorates close to the maximum growth rate as the conditions for the validity of the asymptotics performed on the kinetic theory are violated. The important point concerns however the fact that the model reproduces the large-scale behavior with asymptotic accuracy and displays the correct qualitative behavior when  $b$  is of order unity.

## 5. Concluding Remarks

We have constructed a Landau fluid model that includes small-scale FLR effects in order to reproduce the growth rate of the mirror instability for perturbations with arbitrary transverse wavenumber, and in particular the arrest of the instability at small scales. The model also accurately reproduces the dispersion relation of kinetic Alfvén waves and the phase velocity of transverse magnetosonic waves. At a technical level, an interesting property of this approach concerns the differential form of the closure conditions, which originates from the necessity of approaching the plasma response function by Padé approximants of sufficiently high order to avoid spurious Landau dissipation. A similar development is reported by *Goswami et al.* [2005] in the context of a high order Landau fluid closure for the large-scale dynamics.

The present model should provide an efficient tool to simulate the quasi-transverse dynamics in the nonlinear regime, with the aim to reproduce in particular the formation and evolution of coherent structures and turbulent cascades similar to those observed in the terrestrial magnetosheath by satellite missions (*Sahraoui et al.* [2003] and *Tsurutani et al.* [2005]). Such a study will be the object of a forthcoming paper. Nevertheless, an accurate description of oblique MHD waves requires a closure of the moment hierarchy at a higher order, as illustrated by *Passot and Sulem* [2004a, 2004b] and *Goswami et al.* [2005]. Matching to the kinetic theory as needed to also capture the small-scale dynamics is however a delicate issue that is presently under investigation. Such a refined model would also permit to account for situations where the existence of a strong temperature variations requires a fully nonlinear description of their evolution.

**Acknowledgments.** We acknowledge useful discussions with G. Belmont and F. Sahraoui. This work benefited of support from CNRS program “Soleil-Terre”.

## Appendix

The computation of the velocities and the density fluctuations of the various species require the estimate of  $X_j(\zeta)$  and  $Y_j(\zeta)$  for  $0 \leq j \leq 1$ . For  $l \neq 0$ , one writes  $\zeta_l = -\zeta \frac{l\Omega}{\omega} \left(1 - \frac{\omega}{l\Omega}\right)$ . Using that  $Z(\zeta) = -1/\zeta - 1/2\zeta^3 - 3/4\zeta^5 + O(1/\zeta^7)$  for  $\zeta \rightarrow +\infty$ , one obtains when expanding at the order  $(\omega/\Omega)^3$  needed to get a uniform description of the moments at order  $(\omega/\Omega)^2$ ,

$$X_0 = \frac{\omega}{l\Omega} + \left[1 - \frac{1}{2\zeta_0^2} \left(\frac{T_{\perp}^{(0)}}{T_{\parallel}^{(0)}} - 1\right)\right] \left(\frac{\omega}{l\Omega}\right)^2 + \left[1 - \frac{1}{\zeta_0^2} \left(\frac{T_{\perp}^{(0)}}{T_{\parallel}^{(0)}} - \frac{3}{2}\right)\right] \left(\frac{\omega}{l\Omega}\right)^3 \quad (\text{A1})$$

$$Y_0 = -\frac{1}{2\zeta_0^2} \left(\frac{\omega}{l\Omega}\right)^2 - \frac{1}{\zeta_0^2} \left(\frac{\omega}{l\Omega}\right)^3 \quad (\text{A2})$$

$$X_1 = \frac{1}{2\zeta_0} \left(\frac{T_{\perp}^{(0)}}{T_{\parallel}^{(0)}} - 1\right) \left(\frac{\omega}{l\Omega}\right) + \frac{1}{2\zeta_0} \left(\frac{T_{\perp}^{(0)}}{T_{\parallel}^{(0)}} - 2\right) \left(\frac{\omega}{l\Omega}\right)^2 + \left[\frac{1}{2\zeta_0} \left(\frac{T_{\perp}^{(0)}}{T_{\parallel}^{(0)}} - 3\right) + \frac{3}{4\zeta_0^3} \left(\frac{T_{\perp}^{(0)}}{T_{\parallel}^{(0)}} - 1\right)\right] \left(\frac{\omega}{l\Omega}\right)^3 \quad (\text{A3})$$

$$Y_1 = \frac{1}{2\zeta_0} \left(\frac{\omega}{l\Omega}\right) + \frac{1}{2\zeta_0} \left(\frac{\omega}{l\Omega}\right)^2 + \left(\frac{1}{2\zeta_0} + \frac{3}{4\zeta_0^3}\right) \left(\frac{\omega}{l\Omega}\right)^3. \quad (\text{A4})$$

We are thus led to sum series of the form

$$S_p^k(x) = \sum_{l \neq 0} \frac{1}{l^k} J_l(x) J_{l-p}(x)$$

and

$$\Sigma_p^k(x) = \sum_{l \neq 0} \frac{1}{l^k} J_l'(x) J_{l-p}(x)$$

and to define the integrals

$$C_s^l(b) = \int \tilde{v}_{\perp}^l \Sigma_s^2(\alpha \tilde{v}_{\perp}) e^{-\tilde{v}_{\perp}^2} d\tilde{v}_{\perp}$$

and

$$D_s^l(b) = \int \tilde{v}_{\perp}^l S_s^2(\alpha \tilde{v}_{\perp}) e^{-\tilde{v}_{\perp}^2} d\tilde{v}_{\perp}.$$

One has  $S_0^0(x) = 1 - J_0^2(x)$ ,  $S_1^0(x) = 0$ ,  $\Sigma_0^1(x) = 0$ ,  $S_1^1(x) = -S_{-1}^0 = J_0(x)J_1(x)$ ,  $S_1^1(x) = S_{-1}^1 = \frac{1}{x}(1 - J_0^2(x))$  and  $\Sigma_1^1(x) = \Sigma_{-1}^1 = \frac{1}{x}J_0(x)J_1(x)$ , and one also makes use of the identities  $\int_0^{+\infty} J_0^2(\alpha x) e^{-x^2} x dx = \frac{1}{2}e^{-b}I_0(b)$ ,  $\int_0^{+\infty} J_0(\alpha x) J_0'(\alpha x) e^{-x^2} x^2 dx = \frac{\sqrt{2b}}{4}e^{-b}(I_1(b) - I_0(b))$ ,  $\int_0^{+\infty} J_1^2(\alpha x) e^{-x^2} x^3 dx = \frac{b}{2}e^{-b}(I_0(b) - I_1(b))$ , where  $I_{\nu}(b)$  is the modified Bessel function of order  $\nu$ . One also uses the standard notation  $\Gamma_{\nu}(b) = e^{-b}I_{\nu}(b)$ .

The series  $S_p^k(x)$  and  $\Sigma_p^k(x)$  for  $k \geq 2$  are in contrast difficult to compute exactly but can be estimated with a sufficient accuracy by retaining only the contributions originating from  $l = \pm 1$  and in some cases from  $l = \pm 2$  also. In the expression of  $u_{zp}$ , we approximate  $C_0^2(b)$  by retaining the contributions of  $l = \pm 1$  and  $l = \pm 2$  that are comparable, in the form  $C_0^2(b) \approx$

$(1/4\sqrt{2b})(3b\Gamma_0(b) - 3\Gamma_1(b) - 2\Gamma_1(b) - 2\Gamma_0(b) + 4\Gamma_1(b)/b)$ . For  $D_0^1(b)$ , we only retain the contribution of  $l = \pm 1$ , which gives  $D_0^1(b) \approx \Gamma_1(b)$ . Further contributions are conveniently computed using a software for symbolic calculations. The contribution of  $l = \pm 2$  gives for example  $(1/4b)(b\Gamma_0(b) - 2\Gamma_1(b))$ . One then checks that such corrections do not significantly affect the summation and can be overlooked for the sake of simplicity. Using a similar approximation for coefficients entering  $\chi_{ps}$ , we approximate  $C_1^3(b) \approx (-3b\Gamma_0(b) + 2\Gamma_0(b) + 3b\Gamma_1(b) + 2\Gamma_1(b) - 2\Gamma_1(b)/b + 2\Gamma_0(b)/b - 4\Gamma_1(b)/b^2)/4$  and  $D_1^2(b) \approx (1/\sqrt{2b})(b\Gamma_0(b) - b\Gamma_1(b) - \Gamma_1(b))$ .

The computation of the pressure tensor components in the low frequency limit requires the additional computation of

$$X_2 = \frac{1}{2} \left( \frac{\omega}{i\Omega} \right) + \left[ \frac{1}{2} - \frac{3}{4\zeta_0^2} \left( \frac{T_{\perp}^{(0)}}{T_{\parallel}^{(0)}} - 1 \right) \right] \left( \frac{\omega}{i\Omega} \right)^2 + \left[ \frac{1}{2} - \frac{3}{\zeta_0^2} \left( \frac{T_{\perp}^{(0)}}{T_{\parallel}^{(0)}} - \frac{3}{2} \right) \right] \left( \frac{\omega}{i\Omega} \right)^3 \quad (\text{A5})$$

$$Y_2 = -\frac{3}{4\zeta_0^2} \left( \frac{\omega}{i\Omega} \right)^2 - \frac{3}{2\zeta_0^2} \left( \frac{\omega}{i\Omega} \right)^3. \quad (\text{A6})$$

One also needs the identities

$$S_2^1(x) = S_{-2}^1 = -J_0(x)J_2(x) \quad (\text{A7})$$

$$S_2^2(x) = -S_{-2}^2 = \frac{2}{x} J_0(x)J_1(x) - \frac{2}{x^2} \left( 1 - J_0^2(x) \right) \quad (\text{A8})$$

$$S_2^3(x) = -S_{-2}^3 = -\frac{2}{x^2} J_0(x)J_1(x) + \frac{1}{x} \left( 1 - 2J_1^2(x) \right) \quad (\text{A9})$$

and

$$\int_0^{+\infty} J_0^2(\alpha x) e^{-x^2} x^3 dx = -\frac{1}{2} e^{-b} (bI_0(b) - I_0(b) - bI_1(b)) \quad (\text{A10})$$

$$\int_0^{+\infty} J_2(\alpha x) J_0(\alpha x) e^{-x^2} x^3 dx = \frac{1}{2} e^{-b} (bI_0(b) - I_1(b) - bI_1(b)). \quad (\text{A11})$$

## References

- Akhiezer, A.I., I.A. Akhiezer, R.V. Polovin, A.G. Sitenko, and K.N. Stepanov (1975), *Plasma electrodynamics*, Vol. 1, Pergamon Press.
- Belmont, G. and Mazelle, C. (1992), Polytropic indices in collisionless plasmas: theory and measurements, *J. Geophys. Res.*, *97*, A6, 8327.
- Belmont, G., D. Hubert, C. Lacombe, and F. Pantellini (1992), Mirror mode and other compressible modes, in *Proceedings of the 26th ESLAB Symposium - Study of the solar-terrestrial system, (Killarney, Ireland 16-19 June 1992)*, ESA SP-346, September 1992.
- Bugnon, G., R. Goswami, T. Passot, and P.L. Sulem (2005), Towards fluid simulations of dispersive MHD waves in a warm collisionless plasma, in "Processes in Critical Regions of the Heliosphere", R. Von Steiger & M. Gedalin eds., *Adv. Space Res.* in press.
- Cheng, C.Z. and J.R. Johnson (1999), A kinetic-fluid model, *J. Geophys. Res.*, *104* (A1) 413.
- Chew, G.F., M.L. Goldberger, and F.E. Low (1956), Boltzmann equation and the one-fluid hydrodynamic equations

- in the absence of particle collisions, *Proc. Roy. Soc. (London) A*, *236*, 112.
- Galland Kivelson, M. and D.J. Southwood (1996), Mirror instability II: The mechanism of nonlinear saturation, *J. Geophys. Res.*, *101* (A8), 17365.
- Goswami, P., T. Passot, and P.L. Sulem (2005), A Landau fluid model for warm collisionless plasmas, *Phys. Plasmas*, in press.
- Lacombe, C., F.G.E. Pantellini, D. Hubert, C.C. Harvey, A. Mangeney, G. Belmont, and C.T. Russel (1992), Mirror and Alfvénic waves observed by ISEE 1-2 during crossings of the Earth's bow shock, *Ann. Geophysicae*, *10*, 772.
- Leckband, J.A., D. Burgess, F.G.E. Pantellini, and S.J. Schwartz (1995), Ion distributions associated with mirror waves in the earth's magnetosheath, *Adv. Space Res.*, *15* (8/9), 345.
- McKean, M.E., P. Gary and D. Winske (1992), Mirror and ion cyclotron anisotropy instabilities in the magnetosphere, *J. Geophys. Res.*, *97* (A12), 19421.
- McKean, M.E., P. Gary and D. Winske (1993), Kinetic physics of the mirror instability, *J. Geophys. Res.*, *98* (A12), 21313.
- Mikhailovskii, A.B. and A.I. Smolyakov (1985), Theory of low-frequency magnetosonic solitons, *Sov. Phys. JETP*, *61*, 109.
- Pantellini, P.G.E. (1998), A model of the formation of stable nonpropagating magnetic structures in the solar wind based on the nonlinear mirror instability, *J. Geophys. Res.*, *103* (A3), 4789.
- Passot, T. and P.L. Sulem (2004a), A fluid description for Landau damping of dispersive MHD waves, *Nonlin. Processes Geophys.*, *11*, 245.
- Passot, T. and P.L. Sulem (2004b), A Landau fluid model for dispersive magnetohydrodynamics, *Phys. Plasmas*, *11*, 5173.
- Pokhotelov, O.A., M.A. Balikhin, H. St-C.K. Alleyne and O.G. Onishchenko (2000), Mirror instability with finite electron temperature, *J. Geophys. Res.*, *105* (A2), 2393.
- Pokhotelov, O.A., R.Z. Sagdeev, M.A. Balikhin and R.A. Treumann (2004), Mirror instability at finite-Larmor radius wavelengths, *J. Geophys. Res.*, *109*, A09213, doi:10.1029/2004JA010568.
- Sahraoui, F., Belmont, Pinçon, J.L., Rezeau, L., Balogh, A., Robert, P., and Cornilleau-Wehrin, N. (2004), Magnetic turbulent spectra in the magnetosheath: new insights, *Ann. Geophysicae*, *22*, 2283, S-Ref-ID: 1432-0576/ag/2004-22-2283.
- Sahraoui, F., Belmont, G., Rezeau, L., Pinçon, J.L., Cornilleau-Wehrin, N., and Balogh, A. (2005) Solar wind-Earth coupling: turbulent fragmentation of magnetic structures seen by Cluster, *Phys. Rev. Lett.*, submitted.
- Sahraoui, F., J.L. Pinçon, G. Belmont, L. Rezeau, N. Cornilleau-Wehrin, P. Robert, L. Mellul, J.M. Bosqued, A. Balogh, P. Canu, and G. Chanteur (2003), ULF wave identification in the magnetosheath: The k-filtering technique applied to Cluster II data, *J. Geophys. Res.*, *108* (A9): SMP1,1-18.
- Schwartz, S.J., D. Burgess, and J.J. Moses (1996), Low-frequency waves in the Earth's magnetosheath: present status, *Ann. Geophysicae*, *14*, 1134.
- Smolyakov, A.I., I.O. Pogutse, and A. Hirose (1995), Fluid model of collisionless plasma with finite Larmor radius effects, *Phys. Plasmas*, *2*, 4451.
- Snyder, P.B., G.W. Hammett, and W. Dorland (1997), Landau fluid models of collisionless magnetohydrodynamics, *Phys. Plasmas*, *4*, 3974.
- Southwood, D.J. and M.G. Kivelson (1993), Mirror Instability: I. Physical mechanism of linear instability, *J. Geophys. Res.*, *98* (A6), 9181.
- Stasiewicz, K. (2004), Reinterpretation of mirror modes as trains of slow magnetosonic solitons, *Geophys. Res. Lett.*, *31*, L21804, doi:10.1029/2004GL021282.
- Stasiewicz, K. (2005), Ion-pressure equations derived from measurements in space, *Phys. Rev. Lett.*, *95*, 015004.
- R. A. Treumann, R. A., C. H. Jaroschek, O. D. Constantinescu, R. Nakamura, O. A. Pokhotelov, and E. Georgescu (2004), The strange physics of low frequency mirror mode

turbulence in the high temperature plasma of the magnetosphere, *Nonlin. Processes Geophys.*, *11*, 647, SRef-ID: 1607-7946/npg/2004-11-647.

Tsurutani, B. T., G. S. Lakhina, J. S. Pickett, F. L. Guarnieri, N. Lin, and B. E. Goldstein( 2005), Nonlinear Alfvén waves, discontinuities, proton perpendicular acceleration, and magnetic holes/decreases in interplanetary space and the magnetosphere: intermediate shocks? *Nonlin. Processes Geophys.*, *12*, 321, SRef-ID: 1607-7946/npg/2005-12-321

---

T. Passot, CNRS, Observatoire de la Côte d'Azur, B.P. 4229, 06304 Nice Cedex 4, France (passot@obs-nice.fr)

P.L. Sulem, CNRS, Observatoire de la Côte d'Azur, B.P. 4229, 06304 Nice Cedex 4, France (sulem@obs-nice.fr)

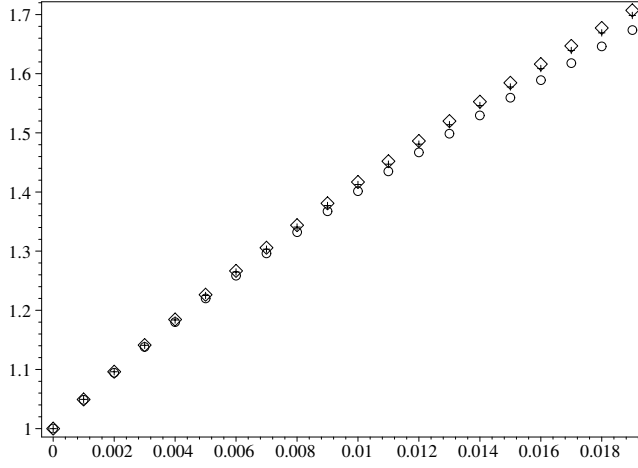


**Figure 1.** Comparison of the normalized frequencies  $\Re(\omega)/k_z v_A$  of kinetic Alfvén waves as a function of  $b$  for  $\beta_{\perp p} = 0.001$ ,  $\tau = 100$  and isotropic equilibrium temperatures, obtained by numerical resolution of the full dispersion relation (circles) and from the analytic formula  $\omega^2 = k_z^2 v_A^2 \left( 1 + \left( \frac{3}{4} + \frac{T_e^{(0)}}{T_p^{(0)}} \right) b \right)$  (diamonds). The cross symbols refer to the predictions of the model described in Section III.

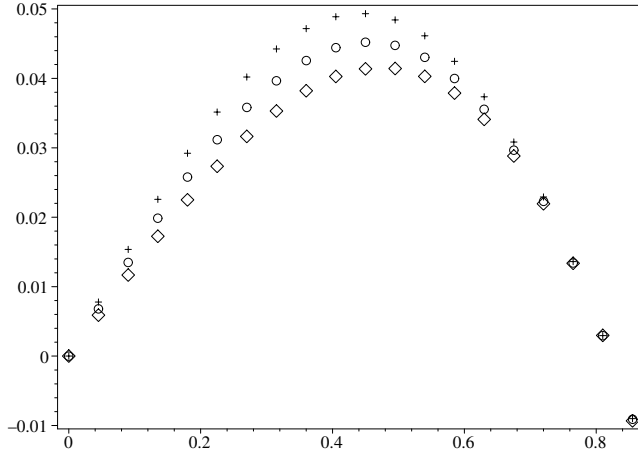


**Figure 2.** Mirror mode growth rate  $\Im(\omega)/k_{\perp}v_{th,p}$  as a function of  $\theta = \frac{k_z}{k_{\perp}}$  for a case with  $A_p = 1$ ,  $A_e = 0.2$ ,  $\tau = 1$ ,  $\beta_{\perp p} = 2$  using the full plasma response function  $R$  (circles) and its one-pole approximation (crosses), together with the growth rate given by formula (23) from Pokhotelov et al. [2000] (diamonds) and based on the “quasi-hydrodynamic approximation” for the large scale dynamics.

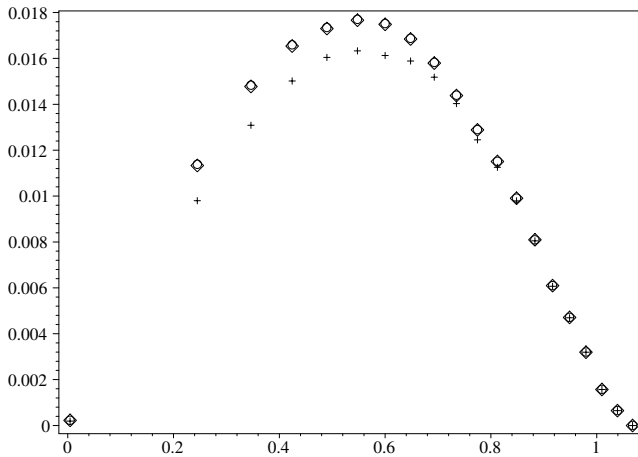


**Figure 3.** Growth rates  $\gamma_{max}/\Omega$  maximized over the angle of propagation, as a function of  $k_{\perp}r_p = \sqrt{2b}$  for  $A_p = \beta_{\perp p} = 1.5$  and cold electrons, using the kinetic dispersion relation calculated with (diamonds) and without (circles) terms in  $\theta^2 = k_z^2/k_{\perp}^2$ . Crosses correspond to the growth rate calculated using a series expansion of the dispersion relation truncated at order  $\zeta^3$  (see text).

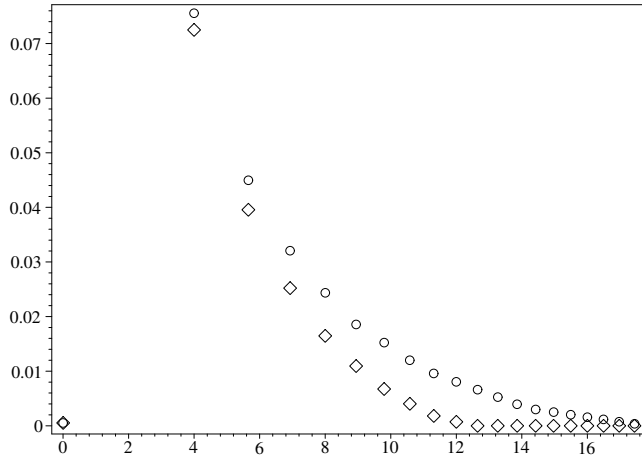


**Figure 4.** Growth rate (maximized over the propagation angles) for electron temperature anisotropies  $A_e = 1$  (diamonds) and  $A_e = 1.005$  (circles), for  $A_p = 1.5$ ,  $\tau = 1$  and  $\beta_{\perp p} = 1.5$ .

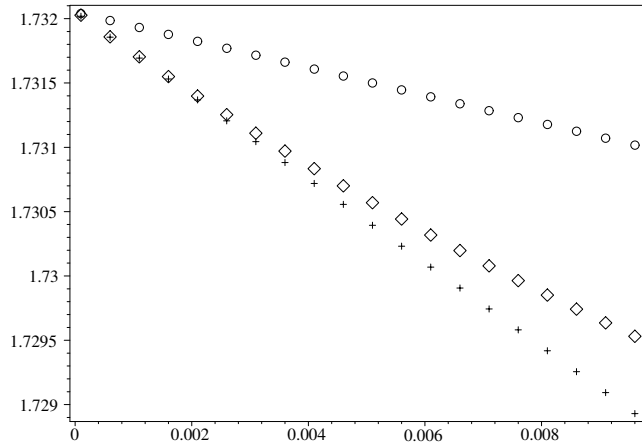


**Figure 5.** Normalized frequencies  $\Re(\omega)/k_{\perp}v_A$  of transverse magnetosonic waves as a function of  $b$  for  $\beta_{\perp p} = 1$ ,  $\tau = 1$  and isotropic equilibrium temperatures, given by numerical resolution of the fluid model (circles), the full kinetic theory (diamond) and by the asymptotic formula of *Mikhailovskii and Smolyakov* [1985] (crosses).



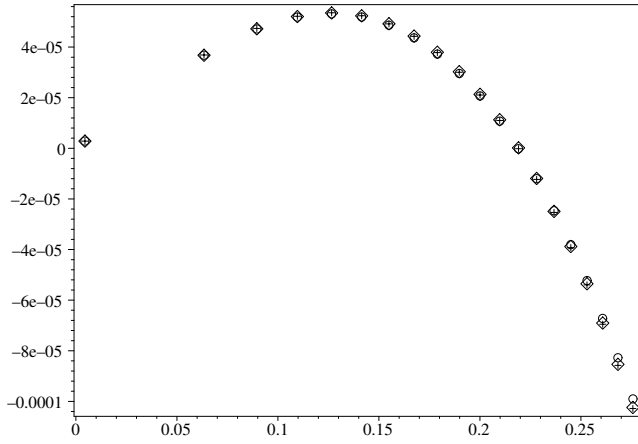


**Figure 6.** Mirror mode growth rates  $\gamma/\Omega$  as a function of  $k_{\perp} r_p = \sqrt{2b}$  for  $\tau = 0$ ,  $A_p = 0.7$ ,  $\beta_{\perp p} = 1.5$ ,  $\theta = 0.1$  obtained from kinetic theory (diamonds) and the fluid model (circles). Crosses correspond to an extended version of the model (see text).

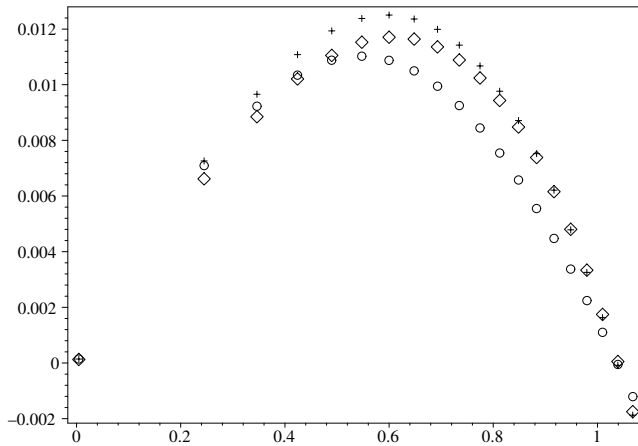


**Figure 7.** Mirror mode growth rates  $\gamma/\Omega$  as a function of  $k_{\perp} r_p = \sqrt{2b}$  for  $\tau = 1$ ,  $A_p = 1.5$ ,  $A_e = 0.1$ ,  $\beta_{\perp p} = 1.5$ ,  $\theta = 0.2$  obtained from kinetic theory (diamonds) and the fluid model (circles). Crosses correspond to a linear model where all terms are kept in the FLR corrections and a fourth pole approximation is used for the plasma response function in the first term of  $\Pi_{yz}$ .